Structural Investigation of Amorphous Europium Metaphosphate by X-ray Diffraction

Mario Cannas, Enrico Manca[a], Gabriella Pinna, Marco Bettinelli[b], and Adolfo Speghini[b]

Dipartimento di Scienze Chimiche, Università di Cagliari, Italy
[a] Dipartimento di Scienze Fisiche, Università di Cagliari, Italy
[b] Istituto Policattedra, Facoltà di Scienze MFN, Università di Verona, Italy

Z. Naturforsch. **53 a,** 919–927 (1998); received August 12, 1998

The local coordination of europium in vitreous Eu metaphosphate has been investigated, using information obtainable from crystalline EuP_3O_9. One glassy sample and one crystalline sample of nominal EuP_3O_9 composition were examined by X-ray diffraction. The description of the close coordination of Eu, deduced from the orthorhombic structure of the crystalline sample, was used as a model for the amorphous situation. Besides, as a monoclinic form of Eu metaphosphate is also reported to exist, a second model was deduced from this structure, starting from the isomorphous monoclinic Yb metaphosphate. Best fitting calculations indicated that orthorhombic coordination is the better model for the short range order of europium in the vitreous metaphosphate.

Introduction

Structural information about the local environment of rare-earth ions in glasses has been the object of many investigations in recent years because the spectral characteristics of these ions undergo modifications depending on the host matrices [1, 2]. In particular, rare-earth ions in phosphate environment have been investigated in view of their potential applications in laser and optoelectronics technologies [1 - 4]. In fact knowledge of the local order around the rare-earth ions and its modifications depending on the sample compositions is essential in order to engineer materials with wanted spectral properties. Pure rare-earth metaphosphate glasses have also been investigated, and they have shown interesting optical properties, coupled with excellent mechanical characteristics and durability. These materials are also interesting for testing the general applicability of recent theoretical models introduced to account for the dynamics of amorphous materials, such as soft potential [5, 6] and phonon-fracton models [7]. Among the rare-earth ions, europium has often been chosen because of the relative simplicity of its optical spectrum.

So far, information on the local structure of cations in metaphosphate rare-earth glasses has been obtained using structural experimental techniques (XRD [8, 9, 11], EXAFS [8, 10], Neutron diffraction [11]) or computer simulations [11, 12], but the results obtained do not give consistent pictures. This fact comes out clearly if we examine the results of two systematic investigations carried out using XRD and EXAFS techniques. X-ray diffraction results describe the local structuring of Pr, Eu and Tb in metaphosphate environment [8,9] as composed by a number of oxygens which increases with decreasing ion size (5.3, 8.5 and 9.2 respectively). The same unusual trend is found for the same three rare-earth cations by EXAFS (coordination numbers equal to 7.1, 7.6, 8, respectively) in an investigation carried out on six rare-earth metaphosphate glasses, a trend which is not confirmed by the entire set of cases examined (Pr, Nd, Eu, Gd, Tb, Ho). In fact, while the coordination distances, hence the ion sizes, decrease regularly with increasing atomic number, as expected for lanthanide elements, the coordination numbers seem to fluctuate randomly between 6 and 10. Besides, even theoretical approaches have failed to provide detailed descriptions of rare-earth coordinations; this has been the case of the "crystal chemistry" analysis [13], which has only been able to predict ranges of coordination values for rare-earth elements in oxide glasses.

With the aim to help in clarifying this matter, we carried out an X-ray diffraction investigation on europium metaphosphate in the vitreous state. A sample

Reprint requests to Prof. M. Cannas; Fax: +39 070 675 4378, E-mail: cannas@vaxca1.unica.it.

0932–0784 / 98 / 1000–0919 $ 06.00

of crystalline EuP_3O_9 was also investigated, with the idea of comparing the local order around the rare-earth ion with that of the amorphous sample.

Sample preparation

Reagent grade Eu_2O_3(Aldrich) and an excess of $(NH_4)_2HPO_4$ (Carlo Erba) were used as starting materials to prepare the amorphous $Eu(PO_3)_3$; after carefully mixing, the powder was melted in an alumina crucible by slow heating (2 °C /min) up to 1700 °C (maximum working temperature of the SiC resistance furnace) and kept at this temperature for 2 h. The melt was rapidly poured on a steel plate at room temperature and covered with a second plate. A few attempts were made to obtain a bubble free, brown, transparent vitreous sample. Possible losses of P_2O_5 at the working temperatures were checked by weighing the cooled melts, but no significant deviations of the weights from the expected values were observed. The sample density, measured by the Archimedes method using xylene as immersion liquid, was 3.35 g/cm^3.

The crystalline $Eu(PO_3)_3$ sample was obtained by heat treatment of the same starting mixture used to prepare the glass. The sample was kept at 1000 °C for 40 h, quenched, milled, mixed again and kept again at 1000 °C for further 24 h. Several attempts were made also in this case to obtain good monophasic crystalline powders.

Structural analysis

X-ray diffraction data on the amorphous sample were collected using $Mo_{K\alpha}$ radiation (λ = 0.71 Å) on a θ–2θ Siemens diffractometer equipped with a graphite monochromator on the diffracted beam. The angular region $4° < 2\theta < 140°$, corresponding to $0.6 < s < 16.0$ Å^{-1}, ($s = [4\pi/\lambda]\sin\theta$, where 2θ is the scattering angle) was divided into 190 intervals using a step scan, preset time method; at least 40,000 counts were collected at each point. The measurements were carried out at room temperature. The observed intensities, corrected for background, absorption and polarisation, were normalised by the semiempirical method proposed by Habenschuss and Spedding [14]. From the normalised intensities I_{eu}, the structure function $i(s)$ was obtained according to

$$i(s) = I_{eu} - \sum_{i=1}^{m} n_i f_i^2(s),$$

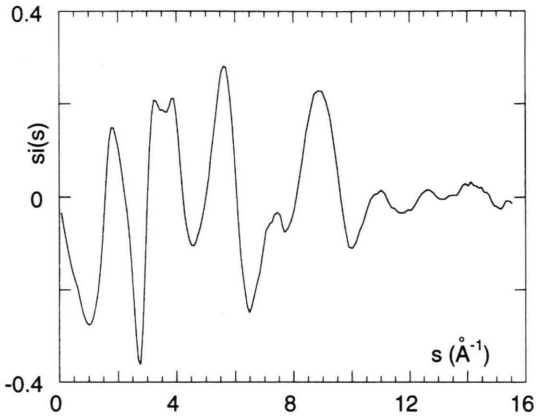

Fig. 1. Experimental structure function of the amorphous sample.

and the Radial Density Function (RDF) was evaluated by Fourier transform

$$G(r) = 1 + \frac{1}{2\pi^2\rho_0 r}\int_{s_{min}}^{s_{max}} s \cdot i(s) \cdot M(s) \cdot \sin(rs) \cdot \mathrm{d}s,$$

where r is the interatomic distance, n_i are the stoichiometric coefficients of the assumed unit containing m atom types, f_i are the scattering factors of the species i, ρ_0 is the average atomic density and $M(s)$ is a modification function of the form

$$M(s) = \frac{\sum n_i f_i^2(0)}{\sum n_i f_i^2(s)} \cdot \exp(-ks^2)$$

with k = 0.005 Å^2. The value of s_{max} = 15 Å^{-1} was used in the Fourier integral. No correction for spurious ripples was applied. The function $si(s)$ is reported in Figure 1. Quantitative structural information can be extracted from the RDF by best fitting model pair contributions to the experimental function. The partial contributions, $g_{ij}(r)$, are defined as gaussian distributions of distances [15]:

$$g_{ij}(r) = \frac{N_{ij}}{4\pi\rho_0 r\sqrt{2\pi r_{ij}\sigma_{ij}}} \cdot \exp\left(\frac{-(r - r_{ij})^2}{2\sigma_{ij}^2}\right),$$

where N_{ij}, r_{ij} and σ_{ij} are the coordination number (i. e., number of j atoms around the origin species i), interatomic distance and its root mean square deviation of the pair ij, respectively. All partial contributions are separately Fourier transformed to reciprocal space, multiplied by the proper weight coefficients

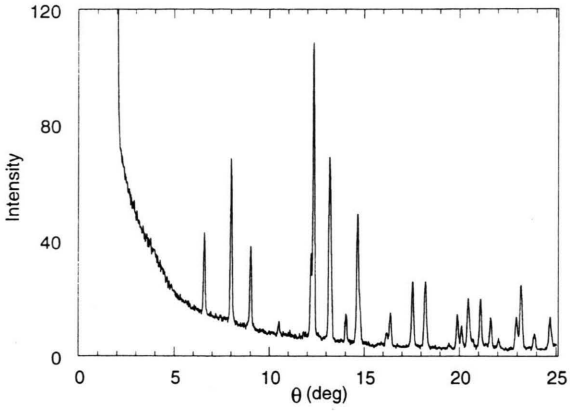

Fig. 2. The X-ray diffraction spectrum of crystalline EuP_3O_9 taken using CuK_α radiation (λ = 1.54 Å).

(function of species concentrations and scattering factors) and summed up into a calculated Total Structure Function, TSF [16]. The TSF is then backtransformed into real space using the same integral cut-offs used in the experimental function, so as to introduce in the model function the same unphysical effects present in the experimental RDF. Model functions can be fitted to the experimental ones using least squares procedures with the structural parameters as independent variables. The calculations are carried out in the reciprocal space, on the TSF functions, though the visualisation of the quality of the fitting results can be made in the real space as well (Peak-Shape analysis [17]). Actually, only the short and medium range interactions can be reconstructed by this method, usually up to the 3 - 3.5 Å distance range in the radial function. Suggestions on the interacting pairs are usually taken from knowledge of chemically and/or structurally similar systems. In the present work we rely on the crystalline state of $Eu(PO_3)_3$.

X-ray data of the crystalline sample were collected using Cu_{K_α} radiation (λ = 1.54 Å) on a θ–θ Seifert diffractometer equipped with a graphite monochromator. Intensities were recorded in the range θ = 2 - 25° by steps of 0.02°. Comparison of the spectrum with those of the known structures of orthorhombic NdP_3O_9 [18] and monoclinic YbP_3O_9 [19] forms showed that it represents an orthorhombic form. It was therefore indexed according to an orthorhombic cell; the unit cell parameters were refined by a program written by Appleman and Evans [20], obtaining the values: a = 11.037(3) Å, b = 8.437(3) Å and c = 7.199(7) Å. Integrated intensities for 34 reflections were then extracted by means of the program EXTRA [21], and the corresponding structure factors were calculated. The experimental spectrum is shown in Figure 2.

Structure analysis was started assuming the fractional coordinates of NdP_3O_9 structure; a few refinement cycles were attempted, conveniently graduating refinable parameters and constraints. However, because of the modest number of independent reflections and of the poor accuracy of some structure factors F_{obs}, caused by partial overlapping and by orientation phenomena, it was not possible to improve much the discrepancy index R with respect to the initial value. The R value taken over a total of 34 reflections came out equal to 0.106, which already means that the structure is correct and went down to 0.082 when 8 reflections with clearly badly estimated F_{obs} values were excluded.

At this point, literature information showed that a second crystalline structure might offer an equally valid model for the simulation of the local order around europium in the vitreous sample. In fact, two crystalline forms are exhibited by metaphosphates of trivalent lanthanide elements: the orthorhombic form, $C222_1$ space group, which is exhibited by metaphosphates of the elements included between lanthanum and gadolinium, and the monoclinic form, $P2_{1/c}$ space group, which is exhibited by metaphosphates of the elements included between samarium and lutetium. Therefore Sm, Eu and Gd metaphosphates crystallise in both forms. As the Eu monoclinic sample was not available, the crystalline structure was obtained on the basis of the unit cell given by Mel'nikov [22]: a = 11.286(8) Å, b = 19.736(16) Å, c = 10.015(7) Å, β = 97.229°(6) and using the fractional coordinates obtained from the isomorphous structure of YbP_3O_9 [19].

The structural differences between the two forms are remarkable:

a) PO_4 tetrahedra form helical chains by corner sharing of two of the oxygen atoms by neighbouring tetrahedra. The repeat units are depicted in Figure 3. In the case of the orthorhombic form (Fig. 3, bottom), the unit is 7.2 Å long and contains a binary axis around which the chain folds; the repeat unit of the monoclinic form (Fig. 3, top) is less twisted and consequently longer, reaching 10.0 Å.

b) In the orthorhombic modification, Eu atoms lie 4.2 Å apart in planar zig-zag chains that run along

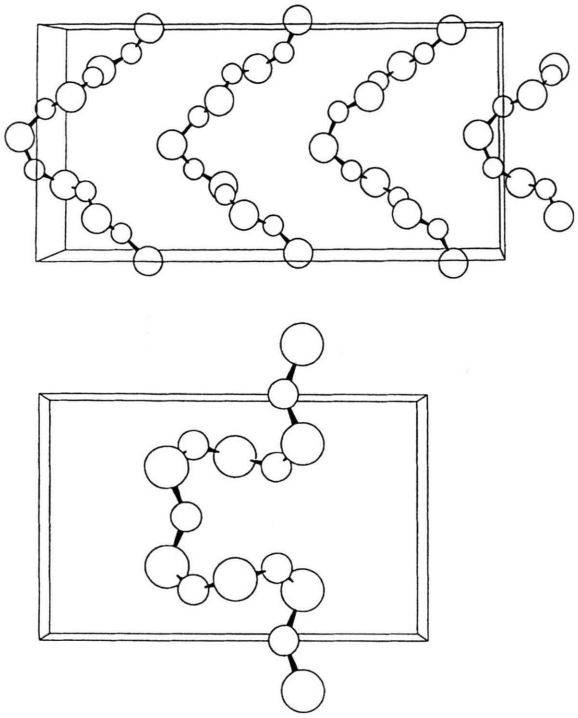

Fig. 3. PO_4 chains in the unit cells of crystalline EuP_3O_9: monoclinic phase (top) and orthorhombic phase (bottom).

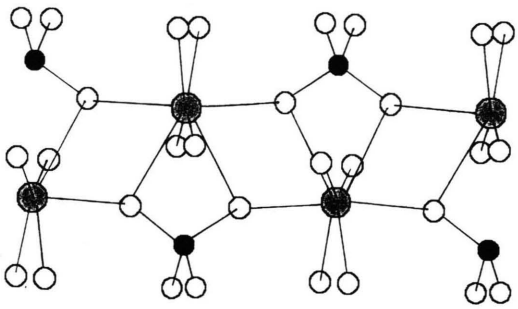

Fig. 4. Chains of edge-connected Eu O_{6+2} polyhedra [Eu: grey circles; P: full circles; O: open circles]. It is evident how the rare-earth ion links together the PO_4 chains which run perpendicularly to the drawing plane.

the crystallographic *c* direction. They are tetracoordinated by asymmetric oxygen bridges, with two oxygens set at a distance of 2.35 Å and two others at 2.64 Å; other four oxygen atoms, located on a perpendicular plane between 2.31 and 2.33 Å, complete a rather irregularly shaped coordination polyhedron. In fact, six vertices are placed in the 2.31 - 2.35 Å range from the central atom forming a distorted octahedron, while the two farthest ones form additional

Table 1. Distances and coordination numbers up to 5 Å of Eu interactions in the crystalline phases of EuP_3O_9.

Pair function	Monoclinic r (Å)	CN	Orthorhombic r (Å)	CN
Eu–O	2.10	2	2.32	4
	2.20	2	2.36	2
	2.30	2	2.64	2
	3.63	1	3.88	2
	3.94	1		
	4.04 - 4.16	3	4.04	2
	4.20 - 4.44	8	4.12	2
			4.32	4
	4.50 - 4.80	9	4.50 - 4.60	8
	4.90 - 5.00	2	4.80 - 4.90	6
		(Total = 30)		(Total = 32)
Eu–P	3.50 - 3.70	6	3.20	1
	4.60 - 5.00	3	3.64	2
			3.76	4
			4.96	4
		(Total = 9)		(Total = 11)
Eu–Eu			4.20	2
	(5.64)	(2)		

bonds of 2.64 Å. A diagrammatic view of these chains is given in Fig. 4, where it can be also seen that contiguous Eu coordination polyhedra share O-O edges. The monoclinic modification contains four crystallographically different coordination polyhedra, each resembling a distorted octahedron, so that the Eu coordination number is only six, with distances Eu-O spread in a range from 2.1 to 2.5 Å. Eu atoms form a sublattice with the unit cell centred on the (100) plane and unit parameters $a' = 1/2\ a$, $b' = 1/3\ b$, $c' = c$, $\beta' = \beta$, the shortest Eu-Eu distance being 5.64 Å. In Table 1, the distances and coordination numbers of Eu interactions in the monoclinic and orthorhombic phases are listed up to the distance of 5 Å.

c) The packing is more compact in the more symmetrical orthorhombic form ($C222_1$) than in the monoclinic one ($P2_1/c$), as reflected in the volume of the $Eu(PO_3)_3$ unit, which is equal to 169 $Å^3$ and 184 $Å^3$ respectively, with corresponding calculated densities of 3.85 g/cm^3 and 3.55 g/cm^3. Therefore the compacting effect due to the sharing of O-O edges in the Eu-O chains prevails on packing restrictions; as a consequence, the higher symmetry $C222_1$ space group is denser than the structure pertaining to the $P2_1/c$ space group, the latter being generally considered as one of the most apt to producing close packings, in accordance with dense packing theories for objects of arbitrary shape [23]. A close examination of the two crystalline structures suggests a reason for this "anomaly":

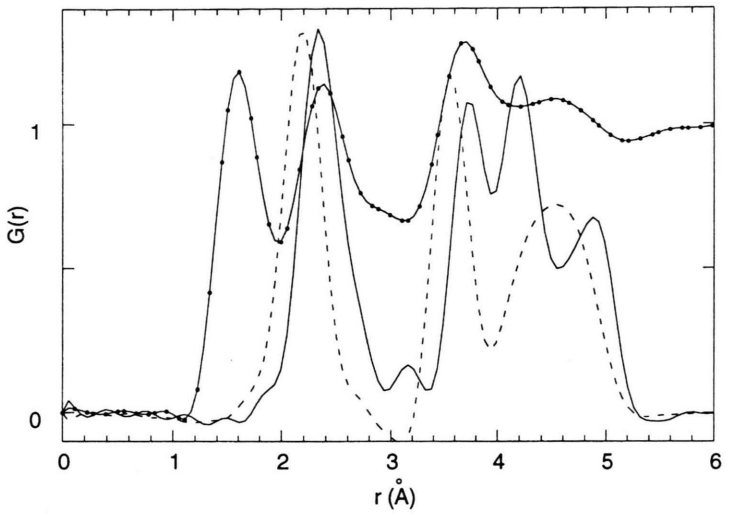

Fig. 5. Experimental radial density function of the amorphous EuP_3O_9 sample (-●-). Model pair contributions g_{ij} (i = Eu, j = O, P, Eu) from the EuP_3O_9 crystalline structures: monoclinic phase (- - -); orthorhombic phase (—); root mean square deviation was assumed constant (σ = 0.1 Å) for all distances.

in the orthorhombic modification, Eu atoms are enclosed in "channels" running along the *c* axis, whereas in the monoclinic phase they lie in the *bc* planes at $a = 0$ and $a = 1/2$. Therefore, the monoclinic form results in a more open structure, with metaphosphate chains arranged so as to form corrugated layers.

Amorphous Fitting

The experimental radial density function $G(r)$ for amorphous $Eu(PO_3)_3$ is plotted in Fig. 5 up to 6 Å. The well resolved first peak in $G(r)$ describes P-O interactions, with an interatomic separation of 1.60 Å expected for a metaphosphate glass system containing rare-earth cations [9]. The Eu-O closest coordination falls under the second peak centered at 2.4 Å, which, however, comprises also O-O interactions coming from the oxygens in the PO_4 tetrahedra. Other features are also evident at longer radial distances: a bump around 3 Å, partially due to the P-P distance within the metaphosphate chains [24], and two other complex peaks centered at 3.7 Å and 4.6 Å. In the attempt to describe quantitatively the short range order around the rare-earth ion, disentangling it from the other terms falling in the same distance range, the information from the two crystalline packing models described above was used to interpret the second peak in the experimental radial function, with the aim to verify whether and which crystalline situation is more consistent with the europium closest coordination in the amorphous state.

Figure 5 also shows the radial features of europium coordination in the orthorhombic structure and in the monoclinic phase superimposed to the glass radial function. The first peaks centered around 2.2 - 2.3 Å are due to first shells composed of oxygen atoms around europium. The second sharp peaks located around 3.6 - 3.7 Å are essentially due to Eu-P interactions. A third broad peak is centered around 4.5 Å in the monoclinic phase and is due to a great number of Eu-O interactions. A different distribution of distances is apparent in the case of the orthorhombic structure in the range 4 - 5 Å, where two sharp peaks are in fact present against the monoclinic broad one; they represent almost the same number of Eu-O interactions, with the addition of some Eu-P second distances around 5 Å; most important, two heavy Eu-Eu contacts fall around 4.2 Å, and are in fact responsible for the sharp feature at that distance. Other minor details further differentiate the two crystalline phases, e. g. a small peak around 3.2 Å due Eu-P closest contacts, which is present in the orthorhombic phase and absent in the monoclinic structure, and important, although barely detectable, two long Eu-O interactions in the orthorhombic phase at 2.64 Å, which affect the right side of the main peak, making it slightly asymmetric. On the whole, the short range structuring of the orthorhombic packing, made up of 6 short distances plus 2 longer ones, appears more similar than the monoclinic structure to the local order of Eu in the glass. Even the peak around 3.7 Å in the glass is better fitted by the Eu-P peak from the orthorhombic structure. Not much can be said about the features beyond

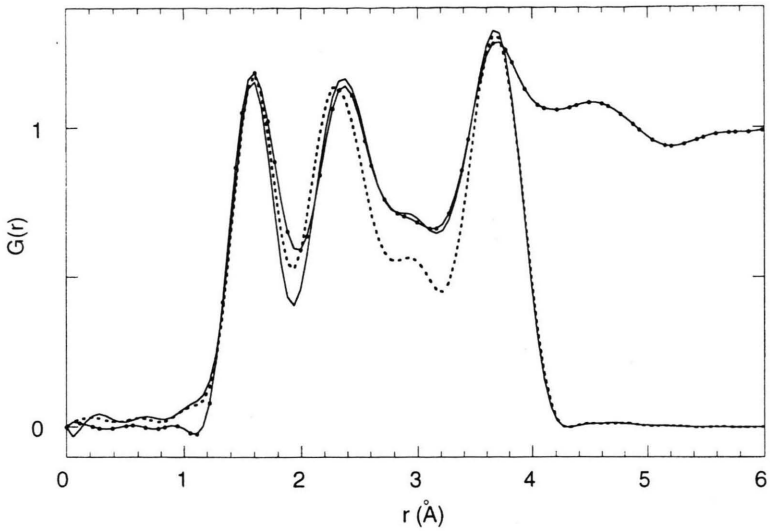

Fig. 6. Fitting of model functions, orthorhombic (—) and monoclinic (- - -), to the experimental one (-•-).

4 Å, not even on the important peak at 4.2 Å due to Eu-Eu interactions, probably useful for Montecarlo or MD simulations, but falling at too long a distance to be helpful here.

For a quantitative evaluation of the two models' ability to describe the short range order of the rare-earth ion in the glass, best fitting procedures may be applied, but not without severe constraints. Therefore, two parallel simulations have been carried out, assuming the same structural description of the phosphate chain up to 3 Å and different short range order around europium. A distribution of distances of the type 4+2 short interactions (between 2.3 and 2.4 Å) and 2 long interactions (around 2.64 Å) was in fact introduced in the orthorhombic simulation, while a distribution of 2+2+2 distances (in the range from 2.1 Å to 2.3 Å) mimicked the monoclinic short range order around europium. One Eu-P interaction was also added around 3.2 Å in the case of the orthorhombic simulation. Other pairs, namely P-O_{II}, O_I-O_{II} and Eu-P, were added in the range 3 - 4 Å, so as to obtain a reasonable description of the left side of the experimental peak centered at 3.7 Å. The maximum variation allowed to the parameters was of about 10% on coordination numbers and of about 4% on distances. The best model functions obtained are reported in Fig. 6; the final parameters are listed in Table 2.

The orthorhombic arrangement around europium still appears better than the monoclinic structuring, although the fitting procedure is clearly not fully exploited. However, a clear discrepancy is present around 1.9 Å in the best case, where the minimum between P-O and Eu-O occurs. Among the possible causes, one is highly probable, that is, the occurrence of short interactions, specifically Al-O, due to the unavoidable presence of small quantities of crucible material. It is a well known fact that molten phosphates are extremely aggressive and dissolve oxides and pure metals [25] even at temperatures much lower than the one (1700 °C) reached by the vitreous sample during preparation. The presence of Al in the glass was actually confirmed by a semi-quantitative analysis carried out on the practically insoluble vitreous sample by X-ray Fluorescence technique: the presence of about 5-6 wt% of Al_2O_3 with respect to the

Table 2. Final parameters describing the model radial density functions from crystalline phases. The functions are reported in Figure 6.

	Monoclinic			Orthorhombic		
Pair function	CN	r (Å)	σ (Å)	CN	r (Å)	σ (Å)
P – O	4.2(2)	1.60(1)	0.12	4.2(2)	1.60(1)	0.12
Eu – O	1.8(2)	2.20(2)	0.20	3.8(2)	2.30(2)	0.16
Eu – O	2.0(2)	2.28(2)	0.20	1.8(2)	2.38(2)	0.15
Eu – O	2.0(2)	2.35(2)	0.12			
Eu – O				2.0(1)	2.81(2)	0.11
O – O	4.3(2)	2.63(2)	0.09	4.1(2)	2.60(2)	0.08
P – P	2.0(1)	3.00(2)	0.12	2.0(1)	3.01(2)	0.09
O – O	3.5(2)	2.95(2)	0.10	3.5(2)	3.05(2)	0.08
Eu – P				1.1(2)	3.26(2)	0.11
O – O	3.5(3)	3.20(3)	0.07	3.5(2)	3.35(2)	0.07
P – O	3.1(2)	3.44(2)	0.07	3.1(2)	3.46(3)	0.08
O – O	2.0(1)	3.55(3)	0.16			
Eu – P	6.0(2)	3.68(5)	0.17	6.1(2)	3.68(2)	0.16
P – O	2.2 (2)	3.66(2)	0.20	2.2(2)	3.80(3)	0.16
P – O	6.0(2)	3.90(2)	0.11	6.1(2)	3.91(3)	0.10

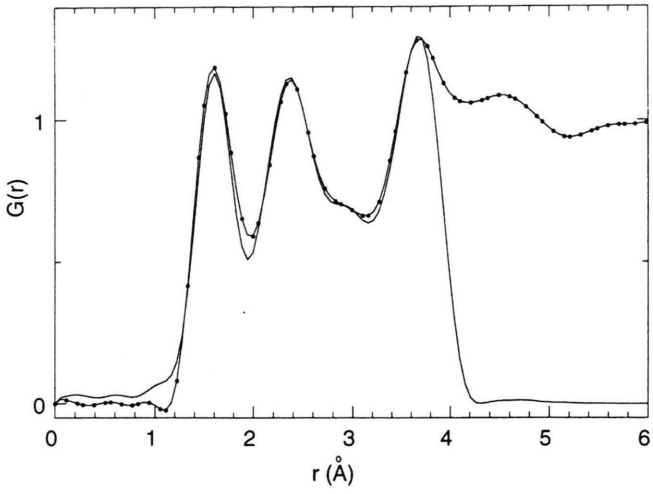

Fig. 7. Best fit function from the orthorhombic model (—) to the experimental one (-•-); Al-O contributions from the alumina of the crucible were also introduced in the simulation.

Table 3. Final coordination parameters for amorphous $Eu(PO_3)_3$ obtained by simulation of the Radial Density Function.

Pair function	CN	r (Å)	σ (Å)
P – O	4.2(2)	1.60(1)	0.12
Al – O	6.2(2)	1.86(1)	0.05
Eu – O	3.9(2)	2.30(2)	0.17
Eu – O	1.8(2)	2.42(2)	0.16
O – O	4.3(2)	2.61(2)	0.12
Eu – O	2.0(1)	2.83(2)	0.15
P – P	2.0(1)	2.96(1)	0.09
O – O	3.5(2)	3.09(3)	0.09
Eu – P	1.1(2)	3.25(2)	0.11
O – O	3.5(2)	3.38(3)	0.08
P – O	3.1(2)	3.49(2)	0.10
Eu – P	6.1(2)	3.68(2)	0.17
P – O	2.2(2)	3.72(3)	0.13
P – O	6.1(2)	3.89(3)	0.11

other oxides was found, while the remaining 95 wt% turned out to give the ratio Eu_2O_3/P_2O_5 = 1/3, thus confirming the metaphosphate composition. A new elaboration of the experimental data using this modified composition did not give rise to a radial function visibly different from the previous one; but the introduction in the model of Al_2O_3 interactions gave rise to a synthetic function which fits better the experimental RDF in the range around 1.9 Å. The final results are reported in Fig. 7 and the best parameter values are given in Table 3.

The best fit distances and coordination numbers were analysed according to the bond valence method [26, 27]. Following it, the valence v_{ij} of a bond between two atoms i and j is so defined that the sum of all the valences of the given atom i with valence V_i obeys the simple law $\sum_j v_{ij} = V_i$; in turn, v_{ij} can be related to the best fit distances d_{ij} by the empirical expression $v_{ij} = [(R_{ij} - d_{ij})/b]$. Here, R_{ij} is the so called bond valence parameter [27], a kind of bond length between atoms i and j averaged over many crystal and molecular structures, and b is commonly taken to be a "universal" constant equal to 0.37 Å. Assuming R_{Eu-O} equal to 2.083 Å [27], the sum taken over 6+2 Eu-O first distances (orthorhombic model) gave the total valence V_{Eu} = 3.17, in excellent agreement with the theoretical value of 3. A similar calculation, carried out for the monoclinic best fit model and therefore taken over 6 Eu-O first distances, gave rise to V_{Eu} = 3.59, thus confirming that the distribution of distances of the orthorhombic model is a better representation of the short range order around europium in vitreous metaphosphate.

Conclusions

A coordination number between 6 and 9 can be expected for the trivalent europium ion on the basis of europium to oxygen size ratio. In fact, using radius values given by Shannon [28] for trivalent europium and two- or three-coordinate oxygen, possible europium coordination numbers of 6, 7, 8, or 9 are obtainable, corresponding to a radius ratio in the range of 0.70 - 0.83. However, this parameter alone cannot give reliable predictions of coordination numbers, because other effects, e. g. steric hindrance from the ligand, can hamper the formation of high coordinations. In fact, in crystalline metaphosphates the anions form infinite chains of corner sharing PO_4 tetra-

hedra. The coordination number of 6 occurs when the non-bridging oxygens are coordinated to only one metal atom, whereas coordination numbers of 7, 8, and 9 are possible if one, or two, or three of these oxygens form bridges between metal atoms. Obviously, the polyphosphate chains would become progressively more constrained and their configurations would drift apart from that of lowest energy. On the other hand, the setting up of more numerous links between cation and ligand would stabilize the whole complex in spite of the constrained configuration of the phosphate chains; the trend towards higher coordinations would then be favoured, up to the point where steric hindrance among the atoms of the chains would make the entire structure unstable. Steric hindrance should therefore be regarded as the critical factor. This is probably the reason why the monoclinic form, with metal coordination of 6, is the most common in crystalline rare-earth metaphosphates, although the orthorhombic form, with coordination number 6+2 also exists for larger cations, europium included. Probably for the same reason, the coordination number of 9 is not found in metaphosphates, but it occurs in lanthanum orthophosphate, where the anions are made up by single PO_4 units [29].

If the situation is complicated in case of crystalline solids, it is not any easier in case of the amorphous state, where many different structural configurations are equally probable. For this reason, we do not even attempt to make predictions, and only limit ourselves to sum up the experimental findings. We underline here that the best configuration of europium coordination in the glass is that similar to the orthorhombic situation, that is 6+2 interactions with oxygens pertaining to the phosphate chains. Relevant points are:

a) The distribution of the six short distances is different from that displayed by the monoclinic structure.

b) The two long distances connect europium with two oxygens, each of which is also linked to another europium through short interaction; long interactions are therefore not equivalent to the short ones and the coordination polyhedron of europium is better viewed as a slightly distorted octahedron, plus two extra long interactions, rather than as a strongly distorted 8-vertices polyhedron.

c) The best fit radial function reported in Fig. 7 and described by the parameters listed in Table 3, shows that essential to the best result is the introduction in the fitting procedure of the heavy term describing one Eu-P interaction around 3.2 Å. This fact gives strong support to the orthorhombic model, as the Eu-P contact is a consequence of the special arrangement between phosphate chains and europium that occurs when some of the oxygens link themselves asymmetrically to two europium atoms.

Probe-sensitive experiments, such as X-ray anomalous scattering carried out using synchrotron radiation of about 50 keV, can produce partial radial distribution functions where only the structural information about one species, namely, the rare-earth cation, is represented. The interpretation of the experimental function is therefore greatly simplified. These experiments lie beyond the scope of this paper and will be the subject of future work.

Acknowledgements

The authors are grateful to Dr. K. Gatterer (TU Graz, Austria) for his help in preparing the glassy europium metaphosphate.

[1] M. J. Weber, J. Non-Cryst. Sol. **47**, 208 (1990).
[2] M. J. Weber in: From Galileo's "Occhialino" to Optoelectronics, P. Mazzoldi Ed., World Scientific, Singapore 1993, p. 332.
[3] S. W. Martin, Eur. J. Solid State Inorg. Chem. **28**, 163 (1991).
[4] J. E. Marion and M. J. Weber, Eur. J. Solid State Inorg. Chem. **28**, 271 (1991).
[5] A. Brodin, A. Fontana, L. M. Börjesson, G. Carini, and L. M. Torell, Phys. Rev. Lett. **73**, 2067 (1994).
[6] G. Carini, G. D'Angelo, G. Tripodo, and G. A. Sanders, Phil. Mag. **71**, 539 (1995).
[7] A. Fontana, G. Carini, A. Brodin, L. M. Torell, M. Börjesson, and G. A. Saunders, Phil. Mag. **71**, 525 (1995).
[8] D. T. Bowron, R. J. Newport, B. D. Rainford, G. A. Saunders, and H. B. Senin, Phys. Rev. B **51**, 5739 (1995).
[9] D. T. Bowron, G. Bushnell-Wye, R. J. Newport, B. D. Rainford, and G. A. Saunders, J. Phys. Condens. Matter **8**, 3337 (1996).
[10] D. T. Bowron, G. A. Saunders, R. J. Newport, B. D. Rainford, and H. B. Senin, Phys. Rev. B **53**, 5268 (1996).

[11] U. Hoppe, R. Kranold, D. Stachel, A. Barz, and A. C. Hannon, Proceedings of NCM7 Conference (Cagliari-Italy, Sept. 1997), J. Non-Cryst. Solids **232 - 234**, 44 (1998).
[12] G. Mountjoy, R. Anderson, J. D. Wicks, D. T. Bowron, and R. J. Newport, Proceedings of NCM7 Conference (Cagliari-Italy, Sept. 1997), published in J. Non-Cryst. Solids **232 - 234**, 227 (1998).
[13] J. Wang, W. S. Brocklesby, J. R. Lincoln, J. E. Townsend, and D. N. Payne, J. Non-Cryst. Solids **163**, 261 (1993).
[14] A. Habenschuss and F. F. Spedding, J. Chem. Phys. **70**, 2797 (1979).
[15] F. Hajdu, Phys. Status Solidi A **60**, 365 (1980).
[16] J. C. De Lima, PHD Thesis, Université de Paris-Sud (1989).
[17] M. Magini, G. Licheri, G. Paschina, G. Piccaluga, and G. Pinna, X-Ray diffraction of ions in aqueous solutions: Hydration and complex formation, CRC Press, Boca Raton, FA, USA 1988, p. 50.
[18] P. Hong, Acta Cryst. B **30**, 468 (1974).
[19] P. Hong, Acta Cryst. B **30**, 1857 (1974).
[20] D. E. Appleman and H. T. Evans, Job 9214: Indexing and least-squares Refinement of Powder Diffraction Data, U. S. Geological Survey, Computer Contribution 20, U. S. National Technical Information Service, Document PB2-16188 (1973).
[21] A. Altomare, G. Cascarano, C. Giacovazzo, A. Guagliardi, A. G. G. Moliterni, M. C. Burla, and G. Polidori, EXTRA: A program for Extracting Structure-factor Amplitudes from Powder Diffraction Data, J. Appl. Cryst. **28**, 842 (1995).
[22] P. P. Mel'nikov, L. N. Komissarova, and T. A. Butuzova, Izv. Akad. Nauk SSSR, Neog. Mater. **17**, 2110 (1981).
[23] A. I. Kitaigorodskii, Organic Chemical Crystallography, Consultants Bureau Enterprises, New York 1961.
[24] W. Matz, D. Stachel, and E. A. Goremychkin, J. Non-Cryst. Solids **101**, 80 (1988).
[25] R. C. Ropp, Inorganic polymeric glasses, Elsevier, Amsterdam 1992, p. 163.
[26] N. E. Breese and M. O'Keeffe, Acta Cryst. B **47**, 192 (1991).
[27] M. O'Keeffe and N. E. Breese, J. Am. Chem. Soc. **113**, 3226 (1991).
[28] R. D. Shannon, Acta Cryst. A **32**, 751 (1976).
[29] D. F. Mullica, W. O. Milligan, D. A. Grossie, G. W. Beall and L. A. Boatner, Inorg. Chim. Acta **95**, 231 (1984).